Scientia Iranica, Vol. 10, No. 4, pp 426–435

SCIENTIA
IRANICA

Coupled Mode Theory of Waveguides with Conducting Interfaces

S. Khorasani[1] and B. Rashidian*

In this paper, the coupling coefficient of two waveguides with conducting interfaces is calculated analytically. It is shown that the control of interface charge densities via a transverse voltage leads to the control of the coupling. To derive the coupling coefficient, the basic Coupled Mode Theory (CMT) with paraxial approximation is improved to include the effect of conducting interfaces. The analysis is performed independently for TE and TM polarizations. Several direct applications of this effect including a multiplexer, a coupler and a modulator/switch and programmable grating are introduced.

INTRODUCTION

The Coupled Mode Theory (CMT) is a well-known and widely used method for analysis of electromagnetic fields in layered media [1-7]. It has been used for analysis of simple [8] and tapered [9,10] optical dielectric waveguides. Improved variations of CMT have been reported for analysis of anisotropic waveguides [11,12] and anisotropic waveguide modulators [13]. Also, CMT in variational form has found applications in the study of optical couplers [14]. CMT has been used in quantum mechanics for analysis of electron wave directional couplers [15] and coupled-cavity lasers [16]. Other studies have considered the extended CMT for grating-assisted codirectional couplers [17] and gain coupled DFB lasers [18]. The analysis of nonlinear waveguide grating using CMT has also been reported in [19]. More recently, an exact CMT for multilayer interference coatings with arbitrary strong index modulations is reported [20]. A valuable review on CMT can be found in [3].

Recently, several applications of layered structures with conducting interfaces, including an integrated optical modulator [21-23], an integrated optical memory and optical transistor [24] and programmable diffractive element [25], have been reported. In these structures, a two-dimensional free interface charge layer is generated at the dielectric interfaces by a transverse voltage, which results in conduction at the interfaces. In general, a conducting interface can be realized through all, or some of, the following effects [26]:

1. The inversion layers in Metal-Oxide-Semiconductor (MOS) structures;
2. The trapped charge in heterojunctions, due to the trapped electron (hole) gas at the edges of conduction (valence) bands, similar to High-Electron-Mobility-Transistors;
3. The depletion layer charge resulting from the initial imbalance between the Fermi levels of the adjacent dielectrics;
4. The trapped charge in the interface traps and interface states and the associated depletion layers.

A report [27] based on Type 2 interface charge has discussed how the propagation of plasma waves in a HEMT can be used to implement a new generation of terahertz devices. Kuijk et al. [28-30] have reported modulators based on Type 3 interface charge in the far-infrared range. Also, experimental verification of transport effects associated with Type 4 interfaces has been recently reported in [26]. Finally, the coupling between waveguides with conducting interfaces has been proposed for implementing programmable gratings in [25,31].

In this paper, CMT is improved to include the effect of the interface charges. The analysis is done

1. *Department of Electrical Engineering, Sharif University of Technology, P.O. Box 11365-9363, Tehran, I.R. Iran.*
*. *Corresponding Author, Department of Electrical Engineering, Sharif University of Technology, P.O. Box 11365-9363, Tehran, I.R. Iran.*

for TE and TM modes separately and closed form expressions are obtained for the resonant coupling modes. The limiting cases of the results are in agreement with the previously reported coupling coefficients.

In the following section, the basis of the CMT is presented. The next section presents the mathematical derivation of coupling coefficients for resonant modes. Then, several numerical examples and typical applications are discussed and, finally, a short conclusion is given.

COUPLED MODE THEORY

In the coupled mode theory it is supposed that the isolated waveguides, which have independent orthogonal modes, become pertubed when coupling occurs [1-7]. For the orthogonality assumption to be applicable, it is necessary for all dielectrics to be lossless. It is pointed out that coupled mode theories based on non-orthogonal modes have also been reported [32], however, the approach in this paper is consistent with the assumption of orthogonality, as follows.

In a recent study, waveguide structures were discussed with purely imaginary interface conductivities in the frequency region of interest, so that all structures were lossless [21]. Therefore, it would be possible to modify the coupled mode theory to include the effect of interface charges without destroying the orthogonality of modes. In order to develop the coupled-mode theory for such structures, an improved transfer matrix method has already been developed to take the effect of interface conductivities into account [33,34]. It is remarkable that based on this approach, a new efficient variational approach for extraction of eigenmodes has been reported in the layered structures being discussed here [35,36].

By expansion of the total field, here denoted by $\mathbf{U}(\mathbf{r})$, in the structure, one can write:

$$\mathbf{U}(\mathbf{r}) = \sum_{m=1}^{n} A_m(z)\mathbf{u}_m(x)\exp(-j\beta_m z), \tag{1}$$

where β_m and $\mathbf{u}_m(x)$ are the propagation constant and the eigenmode of the mth waveguide in the absence of other waveguides, respectively, and $A_m(z)$ is the envelope of the propagating mode across the z-axis, to be found later through coupling equations. The eigenmodes $\mathbf{u}_m(x)$ satisfy:

$$\frac{\partial^2}{\partial x^2}\mathbf{u}_m(x) + \left(n_m^2(x)\frac{\omega^2}{c^2} - \beta_m^2\right)\mathbf{u}_m(x) = 0, \tag{2}$$

where $n_m(x)$ is the refractive index function corresponding to the mth waveguide, in the absence of all other waveguides. Also, in Equation 1, the total field, $\mathbf{U}(\mathbf{r})$, satisfies:

$$\left(\frac{\partial^2}{\partial x^2} + \frac{\partial^2}{\partial z^2} + n^2(x)\frac{\omega^2}{c^2}\right)\mathbf{U}(\mathbf{r}) = 0, \tag{3}$$

where $n(x)$ is the refractive index function of the whole system, representing all waveguides at once.

Insertion of Equation 1 in Equation 3 and using Equation 2 results in:

$$\sum_{m=1}^{n}[n(x)^2 - n_m(x)^2]\frac{\omega^2}{c^2}\mathbf{u}_m(x)A_m(x)e^{-j\beta_m z}$$

$$= \sum_{m=1}^{n} j2\beta_m A'_m(z)\mathbf{u}_m(x)e^{-j\beta_m z}, \tag{4}$$

where the second order derivatives are neglected due to the paraxial approximation. In fact, the paraxial approximation holds for many one- and even two- or three-dimensional optical systems [1,2]. As will be shown, the presence of interface charges, in general, reduces the coupling strength, in further justification of this approximation. In general, if the separation distance between two adjacent waveguides is smaller than the tunneling length of energy outside the guiding layer of the waveguide, then the coupling is no longer weak and the approximation becomes invalid. A quantitative measure for optical tunneling length from film into cladding or substrate layers is given by the Goos-Hänchen shift length [4,5]. For all practical purposes, however, the paraxial approximation can be used and quite often leads to very accurate results [1,2].

According to the orthogonality of modes, one gets:

$$\int_{-\infty}^{\infty} \mathbf{u}_m(x).\mathbf{u}_k{}^*(x)dx \equiv \langle m|k\rangle = 0, \quad m \neq k. \tag{5}$$

Here, the asterisk denotes the complex conjugation. Therefore:

$$\frac{d}{dz}A_k(z) = -\frac{j\omega^2\varepsilon_0\mu_0}{2\beta_k}\langle k|k\rangle^{-1}\sum_{m=1}^{n}\langle k|\Delta n_m^2|m\rangle A_m(z)$$

$$\exp[-j(\beta_m - \beta_z)z], \tag{6}$$

in which $\Delta n_m^2 = n^2 - n_m^2$ is the change in the refractive index of the structure due to the presence of the mth waveguide. In other words, the mth waveguide introduces a perturbation to the overall function of the index of the refraction. Also:

$$\langle k|\Delta n_m^2|m\rangle = \int_{-\infty}^{\infty} \mathbf{u}_k(x).\Delta n_m^2(x)\mathbf{u}_m{}^*(x)dx. \tag{7}$$

By definition, the coupling coefficients are given by:

$$\kappa_{ij} = \frac{\omega^2 \varepsilon_0 \mu_0}{2\beta_i} \langle i|i\rangle^{-1} \langle i|\Delta n_j^2|j\rangle. \tag{8}$$

Therefore, Equation 6 can be rewritten as:

$$\frac{d}{dz} A_k(z) = -j \sum_{m=1}^{k} \kappa_{km} A_m(z) \exp[-j(\beta_m - \beta_k)z], \tag{9}$$

which are the so-called coupled mode equations. In general and within the range of validity of paraxial approximation, the coupled mode Equations 9 can be solved easily to find an exact description of electromagnetic fields. However, it is necessary to compute the coupling coefficients, κ_{ij}, first. The problem is greatly simplified if all the waveguides have an identical propagation constant, say β. Under these situations, the set of Equations 9 can be simplified to:

$$\frac{d}{dz} A_k(z) = -j \sum_{m=1}^{k} \kappa_{km} A_m(z), \tag{10}$$

where the coupling coefficients, κ_{ij}, are:

$$\kappa_{ij} = \frac{\omega^2 \varepsilon_0 \mu_0}{2\beta} \langle i|i\rangle^{-1} \langle i|\Delta n_j^2|j\rangle. \tag{11}$$

COUPLING COEFFICIENTS

In a multilayer dielectric slab waveguide, the presence of interface charges shift the effective index of propagation. This effect has been described in detail for a dielectric waveguide whose interfaces carry free charges [21]. Examples of such structures include quantum-well trapped charges in semiconductor heterostructures [21] and surface state charges on the surface of a semiconductor exposed to vacuum [22].

Note that in contrast to conducting metallic waveguides, the presence of extra free carriers at dielectric interfaces results in a completely different optical effect. In metallic waveguides, eigenmodes are determined solely by geometry and not bulk conductivity, while in dielectric waveguides with conducting interfaces the eigenmodes are influenced by both geometry and finite interface conductivity. As a matter of fact, the interface conductivity has a different physical dimension as well, given by Ω^{-1} and not $\Omega^{-1}\text{cm}^{-1}$, which is the dimension of bulk conductivity. Correspondingly, the effect of interface charges enters the formulation by making the tangential magnetic field discontinuous across the interfaces [21].

Now, the resonant coupling coefficients are derived, as defined in Equation 11, by calculating the resonant modes through the interaction between identical configurations. In this case, only resonant modes

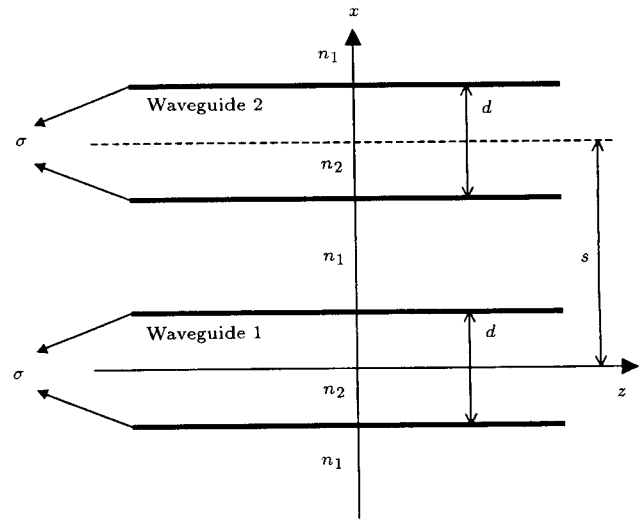

Figure 1. Two-identical waveguides with a displacement between their symmetry axes.

are considered that are guided modes with the same propagation constant. Actually, the coupling between non-resonant modes is usually ignored in coupled-mode analysis of optical structures when a resonant mode exists. The reason is that only coupling between resonant modes with an identical propagation constant is dominant and coupling between non-resonant modes is so weak that it can be ignored [1,2]. On the other hand, the eigenmodes of individual waveguides are functions of their own interface conductivities [21], so that the requirement for having a resonant mode also demands identical interface conductivities. Consequently, the coupling coefficients must be functions of interface conductivities. Results of calculations presented here are shown to be in agreement with this prediction.

A typical structure of two coupled slab waveguides with conducting interfaces is shown in Figure 1. Following the above considerations, both slab waveguides have the same refractive index profiles and interface conductivities, so that the structure has an even symmetry with respect to the symmetry axis at $x = s/2$. Due to different mode behavior and formulations, separate analyses are presented for TE and TM polarizations.

TE Polarization

The eigenmodes are usually normalized by the assumption of total unity radiation power per unit width of the waveguide. Hence, the normalization equation of the TE mode for the mth waveguide is expressed as:

$$\int_{-\infty}^{\infty} \overline{\mathbf{P}}_m(x).\hat{z}dx = -\frac{1}{2} \int_{-\infty}^{\infty} E_{ym}(x) H_{xm}{}^*(x)dx = 1, \tag{12}$$

in which $\overline{\mathbf{P}} = \frac{1}{2}\mathbf{E}\times\mathbf{H}^*$ is the phasor of the time-average Poynting vector. The above can be rewritten as:

$$\int_{-\infty}^{\infty} |E_{ym}(x)|^2 dx = \langle m|m\rangle = \frac{2\omega\mu_0}{\beta}. \tag{13}$$

Now, it is supposed that a symmetric waveguide, with the film thickness of d and the refraction indices $n_2 > n_1$, is given with the z-axis being the symmetry axis. So, the electric field of its eigenmode can be expressed by:

$$E_y(x) =$$

$$\begin{cases} E_3^+ \exp(-jk_1x), & x \geq \frac{d}{2} \\ E_2^+ \exp(-jk_2x) + E_2^- \exp(jk_2x), & -\frac{d}{2} < x < \frac{d}{2} \\ E_1^- \exp(jk_1x), & x \leq -\frac{d}{2} \end{cases}, \tag{14}$$

in which:

$$k_1 = -j\sqrt{\beta^2 - n_1^2\frac{\omega^2}{c^2}}, \tag{15a}$$

$$k_2 = \sqrt{n_2^2\frac{\omega^2}{c^2} - \beta^2}. \tag{15b}$$

Therefore, Equation 13 can be rewritten as:

$$\frac{\beta}{2\omega\mu_0}\int_{-\infty}^{\infty} |E_y(x)|^2 dx = \frac{\beta}{2\omega\mu_0}\int_{-\infty}^{-d/2} |E_1^-|^2 e^{2jk_1x} dx$$

$$+ \frac{\beta}{2\omega\mu_0}\int_{-d/2}^{d/2} |E_2^+|^2 + |E_2^-|^2$$

$$+ 2\mathrm{Re}\{E_2^+ E_2^{-*} e^{-2jk_2x}\}dx$$

$$+ \frac{\beta}{2\omega\mu_0}\int_{d/2}^{\infty} |E_3^+|^2 e^{-2jk_1x} dx = 1. \tag{16}$$

Simplifying Equation 16 gives:

$$\frac{\beta}{2\omega\mu_0}\left\{\frac{e^{-jk_1d}}{2jk_1}\left[|E_1^-|^2 + |E_3^+|^2\right] + d[|E_2^+|^2 + |E_2^-|^2]\right.$$

$$\left. + 2\frac{\sin(k_2d)}{k_2}\mathrm{Re}\left[E_2^+ E_2^-\right]\right\} = 1. \tag{17}$$

Now, if q_{ij} and Δ are the elements and the determinant of the TE transfer matrix, ${}_{\mathrm{TE}}Q_{2\to1}$ [33,34] (c.f. Appendix), it is concluded that:

$$E_2^- = -E_2^+\frac{q_{21}}{q_{22}} \equiv r_{\mathrm{TE}}E_2^+,$$

$$E_3^+ = E_1^- = E_2^+\frac{\Delta}{q_{22}} \equiv t_{\mathrm{TE}}E_2^+. \tag{18}$$

Here, $r = -q_{21}/q_{22}$ and $t = \Delta/q_{22}$ are the reflection and transmission coefficients, respectively, being functions of interface conductivity. Plugging the values of q_{ij} and Δ from Appendix [33,34] in Equation 18 and inserting Equation 18 in Equation 17 gives the following equation for normalized electric field:

$$E_2^+ = \left(\frac{\omega\mu_0}{\beta}\right)^{\frac{1}{2}}\left[\frac{e^{-jk_1d}}{2jk_1}|t_{\mathrm{TE}}|^2 + d + \frac{\sin(k_2d)}{k_2}\mathrm{Re}\{r_{\mathrm{TE}}\}\right]^{-\frac{1}{2}}, \tag{19}$$

where a trivial constant phase factor has been ignored.

It is pointed out that the presence of interface charges with the interface conductivity σ has no effect on the integral in Equation 16; the effect of interface charges indeed enter Equation 19 through the elements of the transfer matrix, q_{ij}. To illustrate this situation, the interface charge layer can be replaced with a dielectric, which has an infinitesimal thickness, δ, and permittivity, $n_2^2\varepsilon_0 - j\sigma/\omega\delta$ [21]. Therefore:

$$\lim_{\delta\to0} -\frac{1}{2}\int_{\pm d/2-\delta/2}^{\pm d/2+\delta/2} E_y(x)H_x^*(x)dx \approx$$

$$\lim_{\delta\to0}\frac{\beta}{2\omega\mu_0}|E_y|^2\delta = 0, \tag{20}$$

where the plus or minus sign, respectively, determines the integration across the upper or lower interface charge sheet. It is assumed that a second identical waveguide, whose symmetry axis is placed at a distance, s, from the symmetry axis of the above waveguide (see Figure 1), has introduced a perturbation to the initial field. The coupling coefficient is given by:

$$k = \frac{\omega\varepsilon_0}{4}\int_{-\infty}^{\infty} E_{y2}\Delta n^2 E_{y1}^* dx, \tag{21}$$

where:

$$\Delta n^2 =$$

$$\begin{cases} n_2^2 - n_1^2 - j\frac{\sigma}{\omega\varepsilon_0}\left[\delta\left(x-s-\frac{d}{2}\right) + \delta\left(x-s+\frac{d}{2}\right)\right], & s-\frac{d}{2} \leq x \leq s+\frac{d}{2} \\ 0, \quad x \leq s-\frac{d}{2}, \quad \text{or}, & x \geq s+\frac{d}{2} \end{cases} \tag{22}$$

Here, $\delta(.)$ represents the Dirac delta and should not be confused with δ in Equation 20. Because of the similarity of waveguides, one has $E_{2y}(x) = E_{1y}(x-s)$

and, thus, the coupling coefficient is obtained as:

$$\kappa = -j\frac{\sigma}{4}t_{\mathrm{TE}}|E_2^+|^2 e^{-jk_1 s}\Big[e^{jk_1\frac{d}{2}}\left(e^{jk_2\frac{d}{2}}+r_{\mathrm{TE}}{}^* e^{-jk_2\frac{d}{2}}\right) + e^{-jk_1\frac{d}{2}}\left(e^{-jk_2\frac{d}{2}}+r_{\mathrm{TE}}{}^* e^{jk_2\frac{d}{2}}\right)\Big] + \frac{\omega\varepsilon_0}{4}(n_2^2-n_1^2)t_{\mathrm{TE}}|E_2^+|^2 \times \left[e^{-jk_2 s}\frac{e^{-j(k_1-k_2)(s+\frac{d}{2})}-e^{-j(k_1-k_2)(s-\frac{d}{2})}}{-j(k_1-k_2)} + r_{\mathrm{TE}}{}^* e^{jk_2 s}\frac{e^{-j(k_1+k_2)(s+\frac{d}{2})}-e^{-j(k_1+k_2)(s-\frac{d}{2})}}{-j(k_1+k_2)}\right]. \tag{23}$$

It should be noted that the computation of Equation 23 is possible by taking Equation 19 into consideration.

When an even symmetry is present in eigenmodes, $\mathbf{E}(x) = \mathbf{E}(-x)$ and r_{TE}=1; so, the above is simplified as:

$$\kappa = -j\sigma t_{\mathrm{TE}}|E_2^+|^2 e^{-jk_1 s}\cos\left(k_2\frac{d}{2}\right)\cosh\left(jk_1\frac{d}{2}\right) + \frac{\omega\varepsilon_0}{2}(n_2^2-n_1^2)t_{\mathrm{TE}}|E_2^+|^2\mathrm{Re} \times \left\{e^{-jk_2 s}\frac{e^{-j(k_1-k_2)(s+\frac{d}{2})}-e^{-j(k_1-k_2)(s-\frac{d}{2})}}{-j(k_1-k_2)}\right\}. \tag{24}$$

Similarly, when the eigenmodes are odd, $\mathbf{E}(x) = -\mathbf{E}(-x), r_{\mathrm{TE}} = -1$ and:

$$\kappa = \sigma t_{\mathrm{TE}}|E_2^+|^2 e^{-jk_1 s}\sin\left(k_2\frac{d}{2}\right)\sinh\left(jk_1\frac{d}{2}\right) + j\frac{\omega\varepsilon_0}{2}(n_2^2-n_1^2)t_{\mathrm{TE}}|E_2^+|^2\mathrm{Im} \times \left\{e^{-jk_2 s}\frac{e^{-j(k_1-k_2)(s+\frac{d}{2})}-e^{-j(k_1-k_2)(s-\frac{d}{2})}}{-j(k_1-k_2)}\right\}. \tag{25}$$

Note that the TE coupling coefficient resulting from even eigenmodes is purely real, while it is purely imaginary between odd eigenmodes (if the interface conductivity, σ, is purely imaginary).

TM Polarization

The computation of TM coupling coefficients is quite similar, with the exception that the normalization condition Equation 12 should be rewritten as:

$$\frac{1}{2}\int_{-\infty}^{\infty} H_{ym}(x)E_{xm}{}^*(x)dx = \frac{\beta}{2\omega\varepsilon_0}\int_{-\infty}^{\infty} n^{-2}(x)|H_{ym}(x)|^2 dx = 1. \tag{26}$$

To compute field amplitudes, the following expansion is employed:

$$H_y(x) = \begin{cases} H_3^+\exp(-jk_1 x), & x \geq \frac{d}{2} \\ H_2^+\exp(-jk_2 x) + H_2^-\exp(jk_2 x), & -\frac{d}{2} < x < \frac{d}{2} \\ H_1^-\exp(jk_1 x), & x \leq -\frac{d}{2} \end{cases}, \tag{27}$$

where:

$$H_2^- = -H_2^+\frac{q_{21}}{q_{22}} \equiv r_{\mathrm{TM}}H_2^+,$$
$$H_3^+ = H_1^- = H_2^+\frac{\Delta}{q_{22}} \equiv t_{\mathrm{TM}}H_2^+. \tag{28}$$

Here, q_{ij} and Δ are the elements and the determinant of the TM transfer matrix, ${}_{\mathrm{TM}}Q_{2\to 1}$ [33,34] (c.f. Appendix). Therefore, the normalization condition results in:

$$H_2^+ = \left(\frac{\omega\varepsilon_0}{\beta}\right)^{\frac{1}{2}}\left[\frac{e^{-jk_1 d}}{2jn_1^2 k_1}|t_{\mathrm{TM}}|^2 + \frac{d}{n_2^2} + \frac{\sin(k_2 d)}{n_2^2 k_2}\mathrm{Re}\{r_{\mathrm{TM}}\}\right]^{-\frac{1}{2}}, \tag{29}$$

where an arbitrary constant phase has been omitted. Relations 23 to 25 can be used by making the replacements $E_2^+ \to H_2^+$ and $\varepsilon_0 \to \mu_0$. Finally:

$$\kappa = -j\frac{\mu_0}{\varepsilon_0}\frac{\sigma}{4}t_{\mathrm{TM}}|H_2^+|^2 e^{-jk_1 s}\Big[e^{jk_1\frac{d}{2}}\left(e^{jk_2\frac{d}{2}}+r_{\mathrm{TM}}{}^* e^{-jk_2\frac{d}{2}}\right) + e^{-jk_1\frac{d}{2}}\left(e^{-jk_2\frac{d}{2}}+r_{\mathrm{TM}}{}^* e^{jk_2\frac{d}{2}}\right)\Big] + \frac{\omega\mu_0}{4}(n_2^2-n_1^2)t_{\mathrm{TM}}|H_2^+|^2 \times \left[e^{-jk_2 s}\frac{e^{-j(k_1-k_2)(s+\frac{d}{2})}-e^{-j(k_1-k_2)(s-\frac{d}{2})}}{-j(k_1-k_2)} + r_{\mathrm{TM}}{}^* e^{jk_2 s}\frac{e^{-j(k_1+k_2)(s+\frac{d}{2})}-e^{-j(k_1+k_2)(s-\frac{d}{2})}}{-j(k_1+k_2)}\right]. \tag{30}$$

For even eigenmodes with $\mathbf{H}(x) = \mathbf{H}(-x)$ and $r_{\mathrm{TM}} = 1$, one gets:

$$\kappa = -j\frac{\mu_0}{\varepsilon_0}\sigma t_{\mathrm{TM}}|H_2^+|^2 e^{-jk_1 s}\cos\left(k_2\frac{d}{2}\right)\cosh\left(jk_1\frac{d}{2}\right) + \frac{\omega\mu_0}{2}(n_2^2 - n_1^2)t_{\mathrm{TM}}|H_2^+|^2\mathrm{Re} \times \left\{e^{-jk_2 s}\frac{e^{-j(k_1-k_2)\left(s+\frac{d}{2}\right)} - e^{-j(k_1-k_2)\left(s-\frac{d}{2}\right)}}{-j(k_1-k_2)}\right\}. \quad (31)$$

while for the odd eigenmodes with $\mathbf{H}(x) = -\mathbf{H}(-x)$ and $r_{\mathrm{TM}} = -1$, it becomes:

$$\kappa = \frac{\mu_0}{\varepsilon_0}\sigma t_{\mathrm{TM}}|H_2^+|^2 e^{-jk_1 s}\sin\left(k_2\frac{d}{2}\right)\sinh\left(jk_1\frac{d}{2}\right) + j\frac{\omega\mu_0}{2}(n_2^2 - n_1^2)t_{\mathrm{TM}}|H_2^+|^2\mathrm{Im} \times \left\{e^{-jk_2 s}\frac{e^{-j(k_1-k_2)\left(s+\frac{d}{2}\right)} - e^{-j(k_1-k_2)\left(s-\frac{d}{2}\right)}}{-j(k_1-k_2)}\right\}. \quad (32)$$

It is seen again that the TM coupling coefficient resulting from the even eigenmodes is purely real, while the coupling coefficient between odd eigenmodes is purely imaginary (if the interface conductivity, σ, is purely imaginary).

EXAMPLES AND APPLICATIONS

To investigate the effect of interface conductivity on the coupling between waveguides, Equation 24 is plotted against the absolute value of σ as shown in Figure 2. Here, the parameters are $\Delta n = 5 \times 10^{-3}, n_1 = 3$ and $s = 2d = 6\lambda = 6\mu$m. These are the same values as used in [1]. The effective index of the propagating guided modes is found by solving the properly modified dispersion equation [21]. As can be observed, the coupling length for zero conductivity is about 2.3 mm, being in agreement with the value reported in [1, p 463].

Here, the coupling length increases with interface conductivity. The main reason for this behavior could be related to the dramatic decrease of the transmission coefficient, t_{TE}, in Equation 24; indeed, in the limit of infinite interface conductivity, one has $t_{\mathrm{TE}} = 0$. The more the interface conductivity, the more confined the guided mode.

To clarify the argument, the field profiles of two waveguides have been plotted in Figure 3a for TE_0 eigenmodes in the absence of interface charges.

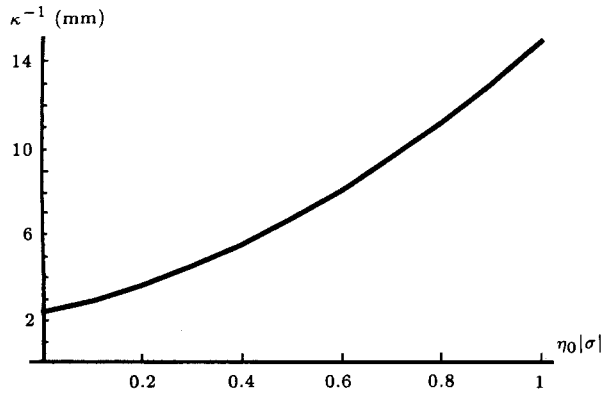

Figure 2. The TE coupling length κ^{-1} vs the absolute value of interface conductivity ($s = 6$ μm).

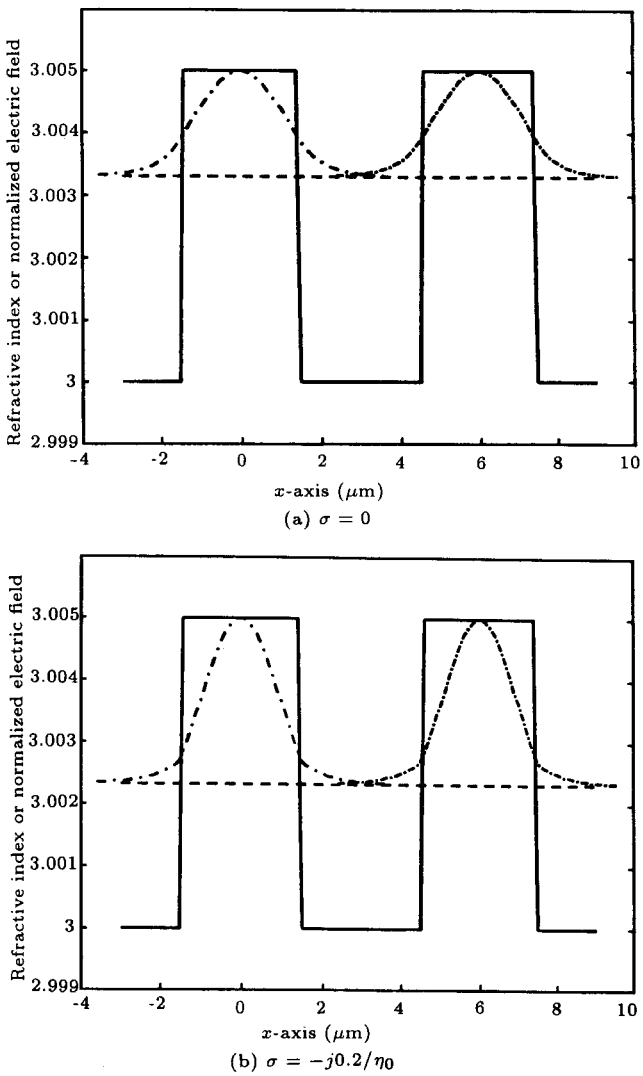

Figure 3. The TE_0 mode profiles of two adjacent waveguides (dashed curves). As can be seen, the modes are better confined in the presence of interface charges. The horizontal dashed line represents the normalized propagation index $\lambda\beta/2\pi$. Solid curves show the profile of refractive index for two waveguides.

Here, the solid curve shows the profile of refractive index corresponding to two waveguides and the horizontal dashed line represents the normalized propagation constant, $\lambda\beta/2\pi$, which has been found to be 3.0033. In Figure 3b, calculations are done for the same structure but with an interface conductivity of $\sigma = -j0.2/\eta_0$. The normalized propagation constant, $\lambda\beta/2\pi$, here has shifted down to 3.0023. While the electric field is continuous, its derivative is not. The reason is that the derivative of the electric field describes the tangential magnetic field, which is discontinuous due to the interface current induced by the tangential electric field (see Appendix). As a result, the evanescent tail of the electric field decays more rapidly outside the film layer and the modes are better confined.

Therefore, the second waveguide is less affected by the guided wave propagating in the first, so the coupling length increases. Meanwhile, the interface conductivity shifts the propagating effective index so that more energy is confined within the bulk of film layer. This phenomenon behaves differently for larger distances between waveguides, as plotted in Figure 4 ($s = 10\mu$m). Contrary to expectation, the coupling length initially decreases, reaching a minimum at about $\sigma = -j0.25/\eta_0$ and then starts increasing.

This unusual behavior can be explained as follows: Interface conductivity has two different effects on the guided and coupled modes. The first leads to the better confinement of modes in the waveguide, which results in increasing the coupling length (as in Figure 2). The reason is that the magnitude of transmission coefficient decreases with increasing the interface conductivity, as just described above. Consequently, the second waveguide is more inclined to steal energy from the evanescent tail of the guided propagating mode of the first waveguide, resulting in a decrease in coupling length. These two mechanisms compete with each other, so that a behavior shown in Figure 4 results.

Figure 5 shows the variation of TM coupling length with interface conductivity. It is observed that in the absence of interface conductivity, the value of 21 mm is obtained for the coupling length, being about 9 times larger than that of TE mode. This is due to the small refractive index contrast of the waveguide, resulting in a weaker coupling of the TM modes. Compared to Figure 2, the coupling length is also increasing, but at a much higher rate. Increasing the separation between the waveguides to 10μm, as plotted in Figure 6, does not change the general behavior, contrary to the TE mode. The reason behind this difference could be explained by noting that the presence of interface charges introduces an abrupt drop in the profile of the magnetic field. Therefore, TM modes enjoy a better confinement compared to TE modes. The competing mechanism is, however, too weak to introduce a decrease in the coupling length.

An immediate conclusion of the above discussions

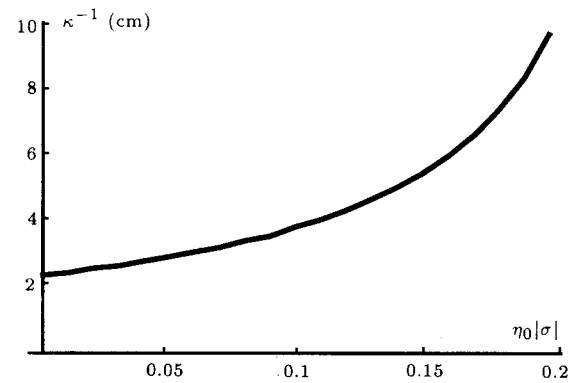

Figure 5. The TM coupling length κ^{-1} vs the absolute value of interface conductivity ($s = 6$ μm).

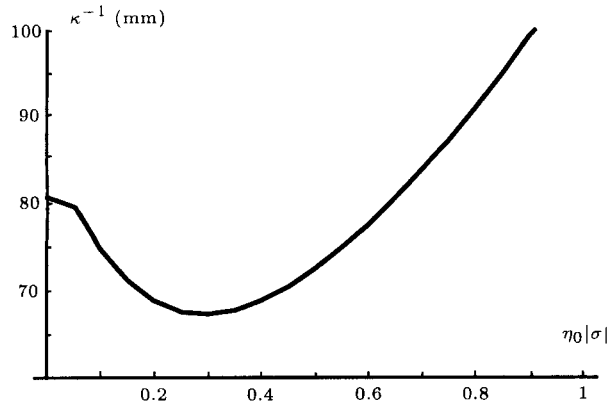

Figure 4. The TE coupling length κ^{-1} vs the absolute value of interface conductivity ($s = 10$ μm).

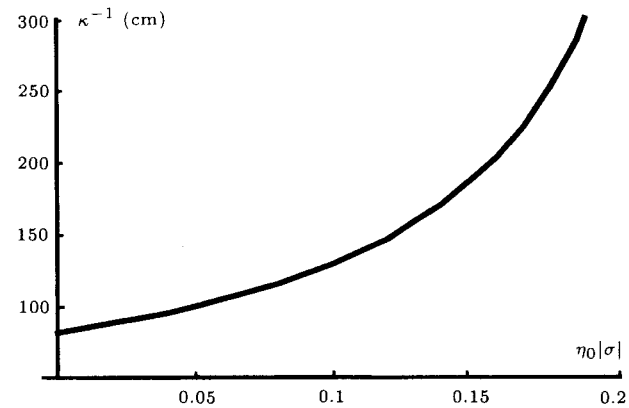

Figure 6. The TM coupling length κ^{-1} vs the absolute value of interface conductivity ($s = 10$ μm).

is the feasibility of a programmable optical coupler. As a general rule, the coupling length between two waveguides can be controlled by controlling the density of interface charges. The controlling mechanisms can have quite different natures [21,26], depending on the physical origin of the interface charges, as classified in the introduction. In practice, it is easy to obtain charge densities as high as 3×10^{13} cm^{-2} across the interfaces of large bandgap semiconductors. Still larger charge densities can be obtained in the depletion layers of highly doped $p - n$ junctions. However, surface state interface charges usually have much lower densities and are limited to 5×10^{11} cm^{-2} [22].

By extension of this structure and using single mode waveguides, a Mach-Czhender-like [37] optical switch or modulator can be constructed. Therefore, by stacking the waveguides and keeping independent control on the interface charges of each waveguide, a multiplexer results. Furthermore, if the structure is allowed to become periodic, a programmable grating is obtained, whose mode diffraction efficiencies, polarizations and even directions can be controlled. This idea and further application in novel optical devices are explained in detail elsewhere [38,39].

CONCLUSIONS

The coupled mode theory has been improved to take the effect of conducting interfaces into account. Closed form expressions for the coupling coefficient of identical symmetric waveguides have been found separately for TE and TM modes. The results show that the coupling becomes generally weaker when the interface conductivity is increased. Applications such as in modulators, switches, multiplexers and programmable gratings have been remarked.

REFERENCES

1. Yariv, A. and Yeh, P., *Optical Waves in Crystals*, John Wiley & Sons, New York, chap. 11 (1984).
2. Yariv, A. "Coupled-mode theory for guided-wave optics", *IEEE J. Quantum Electron.*, **QE-9**, pp 919-933 (1973).
3. Huas, H.A. and Huang, W. "Coupled-mode theory", *Proc. IEEE*, **79**, pp 1505-1518 (1991).
4. Kogelink, H., *Integrated Optics*, Tamir, T., Ed., Springer-Verlag, Berlin, Germany (1975).
5. Kogelink, H., *Guided-Wave Optoelectronics*, Tamir, T., Ed., Springer-Verlag, Berlin, Germany (1990).
6. Huang, W.P., Chu, S.T. and Chaudhuri, S.K. "A scalar coupled-mode theory with vector correction", *IEEE J. Quantum Electron.*, **QE-28**, pp 184-193 (1992).
7. Tzolov, V.P., Feng, D., Tanev, S. and Jakubczyk, Z.J. "Modeling tools for integrated optical and fiber devices", *Proc. SPIE*, **3620**, pp 162-173 (1999).
8. Vassallo, C. "About coupled-mode theories for dielectric waveguides", *J. Lightwave Technol.*, **LT-6**, pp 294-303 (1988).
9. Huang, W.P. and Haus, H.A. "Self consistent vector coupled-mode theory for tapered optical coupler", *J. Lightwave Technol.*, **LT-8**, pp 922-926 (1990).
10. Lessard, S. and Huang, W. "Assessment of coupled-mode theory for tapered optical coupler", *J. Lightwave Technol.*, **LT-11**, pp 405-407 (1993).
11. Tsang, L. and Chuang, S.L. "Improved coupled-mode theory for anisotropic waveguides", *J. Lightwave Technol.*, **LT-6**, pp 304-311 (1988).
12. Tian, F., Gao, F., Yizun, W. and Peida, Y. "Improved coupled-mode theory of anisotropic optical waveguides", *IEEE J. Quantum Electron.*, **QE-25**, pp 249-251 (1989).
13. Tian, F., Wu, Y.Z. and Ye, P.D. "Improved coupled-mode theory for anisotropic waveguide modulators", *IEEE J. Quantum Electron.*, **QE-24**, pp 531-536 (1988).
14. Huang, W. and Chaudhuri, S.K. "Variational coupled-mode theory of directional couplers", *J. Lightwave Technol.*, **LT-8**, pp 1565-1570 (1990).
15. Sarangan, A.M. and Wei-Ping, H. "A coupled-mode theory for electron wave directional couplers", *IEEE J. Quantum Electron.*, **QE-30**, pp 2803-2810 (1994).
16. Lang, R.J. and Yariv, A. "An exact formulation of coupled-mode theory for coupled-cavity lasers", *IEEE J. Quantum Electron.*, **QE-24**, pp 66-72 (1988).
17. Abiri, H., Bakhtazad, A. and Rahnavard, M.H. "Extended coupled-mode theory for grating-assisted codirectional couplers", *Proc. SPIE*, **2399**, pp 109-117 (1995).
18. Khaleghi, F., Simova, E.S. and Kavehrad, M. "All-optical tunable filter in a nonlinear waveguide grating: analysis using coupled-mode theory", *Proc. SPIE*, **2402**, pp 9-17 (1995).
19. Zakery, A. and Bakhtazad, A. "New coupled-mode analysis of gain coupled DFB lasers", *Proc. SPIE*, **2886**, pp 213-224 (1996).
20. Matuschek, N., Kartner, F.X. and Keller, U. "Exact coupled-mode theories for multilayer interference coatings with arbitrary strong index modulations", *IEEE J. Quantum Electron.*, **QE-33**, pp 295-302 (1997).
21. Khorasani, S. and Rashidian, B. "Guided wave propagation in dielectric slab waveguide with conducting interfaces", *J. Opt. A: Pure Appl. Opt.*, **3**(5), pp 380-386 (2001).
22. Darabi, E., Khorasani, S. and Rashidian, B. "optical modulation by surface states", *Semicond. Sci. Technol.*, **18**(1), pp 60-67 (2003).

23. Khorasani, S., Nojeh, A. and Rashidian, B. "Design and analysis of the integrated plasma wave micro-optical modulator/switch", *Fiber Int. Opt.*, **21**, pp 173-191 (2002).

24. Khorasani, S., Nojeh, A. and Rashidian, B. "A new integrated optical memory based on the plasma wave modulator/switch", *Proc. SPIE*, **4277**, pp 311-314 (2001).

25. Rashidian, B. and Khorasani, S. "A new integrated programmable optical diffractive element", *Proc. SPIE*, **4277**, pp 428-434 (2001).

26. Khorasani, S., Motieifar, A. and Rashidian, B. "Dynamics of interface traps in bonded silicon wafers", *Semicond. Sci. Technol.*, **17**(5), pp 421-426 (2002).

27. Dyakonov, M.I. and Shur, M.S. "Plasma wave electronics: Novel terahertz devices using two dimensional electron fluid", *IEEE Trans. Electron Dev.*, **43**, pp 1640-1645 (1996).

28. Kuijk, M. and Vounckx, R. "Use of two-dimensional electron gas in optical information processing: Proposal for integrated mirror optical switch", *Electron. Lett.*, **25**, pp 231-233 (1989).

29. Steins, J., Kuijk, M., Vounkcx, R. and Borghs, G. "New modulator for far-infrared light: Integrated mirror optical switch", *Appl. Phys. Lett.*, **59**, pp 3210-3212 (1991).

30. Kuijk, M. and Vounckx, R. "Optical plasma resonance in semiconductors: Novel concepts for modulating far-infrared light", *J. Appl. Phys.*, **66**, pp 1544-1548 (1989).

31. Rashidian, B. and Khorasani, S. "Design and analysis of the plasma wave based programmable grating", *Proc. SPIE*, **4598**, pp 175-185 (2001).

32. Huang, W. and Lit, J.W.Y. "Nonorthogonal coupled-mode theory of grating-assisted codirectional couplers", *IEEE J. Quantum Electron.*, **QE-28**, pp 184-193 (1992).

33. Khorasani, S. and Rashidian, B. "Modified TMM for slab waveguides with conducting interfaces", *Proc. SPIE*, **4580**, pp 167-169 (2001).

34. Khorasani, S. and Rashidian, B. "Modified transfer matrix method for conducting interfaces", *J. Opt. A: Pure Appl. Opt.*, **4**(3), pp 251-256 (2002).

35. Khorasani, S., Mehrani, K. and Rashidian, B. "Efficient variational approach to propagation eigenmodes in layered waveguides", *Proc. SPIE*, **4646**, pp 669-673 (2002).

36. Mehrany, K., Khorasani, S. and Rashidian, B. "Variational approach for extraction of eigen-modes in layered waveguides", *J. Opt. Soc. Am. B*, **19**(9), pp 1978-1981 (2002).

37. Ghatak, A.K. and Thyagarajan, K., *Optical Electronics*, Cambridge University Press, Cambridge, p 445 (1989).

38. Khorasani, S., Nojeh, A. and Rashidian, B. "Programmable grating based on the interface charge control", *Proc. SPIE*, **4640**, pp 255-260 (2002).

39. Mehrany, K., Khorasani, S. and Rashidian, B. "Novel optical devices based on surface wave excitation at conducting interfaces", *Semicond. Sci. Tech.*, **18**, pp 582-588 (2003).

APPENDIX

Transfer Matrices

Suppose that a layered structure is composed of $l+2$ slabs with refractive indices $n_m = (\varepsilon_m/\varepsilon_0)^{1/2} (m = 1 \cdots l+2)$ having $l+1$ interfaces normal to the x-axis at $X_m (m = 1 \cdots l+1)$ and a wave which is propagating along the positive direction of z-axis so the y-component of the wavevectors is zero. The mth interface is allowed to have an interface conductivity, σ_m, so that the tangential component of the electric field across the interface produces a proportional interface current density as follows:

$$\mathbf{J}_m(z) = \sigma_m[\hat{x} \times \mathbf{E}_m(X_m, z)] \times \hat{x}, \tag{A1}$$

where $\mathbf{E}$ stands for the electric field vector. It should be noted that the dimension of the interface conductivity, σ_m, is equal to $\Omega^{-1} = A/V$, being different from the bulk conductivity. Correspondingly, the dimension of $\mathbf{J}$ is A/m. It is convenient to describe the field distribution in the mth dielectric by a linear combination of two plane waves as follows:

$$\mathbf{U}_m(x,z) = (\mathbf{U}_m^+ e^{-jk_m x} + \mathbf{U}_m^- e^{+jk_m x}) \exp(-j\beta z), \tag{A2}$$

where $\mathbf{U}$ represents the electric or magnetic field vectors $\mathbf{E}$ or $\mathbf{H}$ and $\mathbf{U}^+$ and $\mathbf{U}^-$ are constant complex phasors representing the up and down travelling waves, respectively. The presence of conduction at the interface has no effect on the basic reflection and refraction mechanisms as discussed in [21], so that the Snell law for angles is applicable.

Continuity of the tangential electric field at the mth interface with $x = X_m$, reads $(m = 1 \cdots l+1)$;

$$\mathbf{E}_m(X_m, z) \times \hat{x} = \mathbf{E}_{m+1}(X_m, z) \times \hat{x}, \tag{A3}$$

while the tangential magnetic field is discontinuous across the interface as [32,33]:

$$[\mathbf{H}_m(X_m, z) - \mathbf{H}_{m+1}(X_m, z)].(\hat{x} \times \hat{e})\hat{e} = \mathbf{J}_m, \tag{A4}$$

where $\hat{e}$ is a unit vector parallel to $\mathbf{J}_m(z)$. These boundary conditions can be simplified when the electric or magnetic field has a y component only, which refers to $\hat{e} = \hat{y}$ for TE and $\hat{e} = \hat{z}$ for TM modes, respectively.

Applying the interface conditions together with Equation A2 results in solutions of the form:

$$\begin{bmatrix} \mathbf{U}_{m+1}^{+} \\ \mathbf{U}_{m+1}^{-} \end{bmatrix} = Q_{m \to m+1} \begin{bmatrix} \mathbf{U}_{m}^{+} \\ \mathbf{U}_{m}^{-} \end{bmatrix}. \tag{A5}$$

Here, $Q_{m \to m+1}$ is referred to as the transfer matrix from the mth to the $m+1$th layer, given by [32,33]:

$${}_{\mathrm{TE,TM}}q_{i,j}^{m} = \frac{{}_{\mathrm{TE,TM}}p_{i,j}^{m}}{2k_{m+1}} \exp \times \{-j[(-1)^{i}k_{m+1} - (-1)^{j}k_{m}]X_{m}\}, \tag{A6}$$

in which:

$${}_{\mathrm{TE}}p_{i,j}^{m} = k_{m+1} + (-1)^{i+j}k_{m} + (-1)^{i}\omega\mu_{0}\sigma_{m}, \tag{A7a}$$

$${}_{\mathrm{TM}}p_{i,j}^{m} = k_{m+1} + (-1)^{i+j}\frac{\varepsilon_{m+1}}{\varepsilon_{m}}k_{m} + (-1)^{j}\frac{\sigma_{m}}{\omega\varepsilon_{m}}k_{m}k_{m+1}. \tag{A7b}$$